

## The asymmetric effect of plasma response to variation of quasar radiation

ZHICHENG HE<sup>1,2</sup> AND TINGGUI WANG<sup>1,2</sup>

<sup>1</sup>CAS Key Laboratory for Research in Galaxies and Cosmology, Department of Astronomy, University of Science and Technology of China, Hefei, Anhui 230026, China

<sup>2</sup>School of Astronomy and Space Science, University of Science and Technology of China, Hefei, Anhui 230026, China

### ABSTRACT

Plasma is prevalent throughout the universe. The cosmic plasma serves as not only a crucial tracer for studying the evolution of the cosmos but also an ideal laboratory for investigating the properties of plasma in extreme conditions. As one of the important contributors to the re-ionization of the universe, the variability in quasar (driven by the supermassive black hole) radiation presents a convenient opportunity to study the response of gases ionized by them. Based on extensive statistical analysis using data from the Sloan Digital Sky Survey (SDSS), it has been demonstrated that the response of gases to quasar radiation exhibits asymmetry. Specifically, over 70% of broad absorption lines (BALs) gas in quasar host galaxies exhibit a negative response. Through analytical calculations and photoionization simulations of C IV, we found that the response of gases to radiation is asymmetric for low and high ionization states. In high ionization states, the response time scale is shorter, leading to the detection of more negative responses. In actual case, the observation time interval is mostly greater than 1 day, and hence the asymmetric effect of the C IV response gives a typical gas density of upper limit of  $10^7 \text{ cm}^{-3}$ . Interestingly, this is consistent with the fact that most of the measured BAL gas densities are below  $10^7 \text{ cm}^{-3}$ . In principle, the detection of this asymmetric effect becomes easier with lower plasma density or shorter observation time intervals.

*Keywords:* Plasma astrophysics–Photoionization–Recombination–Quasar absorption line spectroscopy

### 1. INTRODUCTION

Plasma, consisting of ionized particles, is prevalent in the universe, at high redshifts ( $z > 1100$ ) and after the cosmic reionization epoch with  $z < 6$  (Barkana & Loeb 2001; Kriss et al. 2001; Zheng et al. 2004; Fan et al. 2006; Tilvi et al. 2020; Yung et al. 2020). Astrophysical plasma, found in entities such as the interstellar medium (ISM) and intergalactic medium (IGM), serves as a valuable tool for exploring the evolutionary processes of both the universe and celestial bodies. Simultaneously, cosmic celestial bodies provide an ideal laboratory for studying the principles of plasma physics in extreme situations such as extremely high temperatures or low densities. Quasars, a class of high luminosity active galactic nuclei (AGN), fueled by the accretion disk of supermassive black holes (SMBHs), stand out as the most luminous and persistent celestial objects in the universe, with their redshift frontier extending to approximately  $z \sim 7.6$  (Wang et al. 2021). Quasars is believed to play crucial roles in both cosmic reionization (Jakobsen et al. 1994; Loeb & Barkana

2001; Fan et al. 2023) and the evolution of galaxies (Fabian 2012; Kormendy & Ho 2013; Veilleux et al. 2020), through the intense ionizing radiation and enormous energy released outward.

The radiation of quasar typically displays aperiodic variabilities, often described by the damped random walk (DRW) model (Kelly et al. 2009). The variability in quasar radiation presents a convenient opportunity to study the response of gases ionized by them. The ionization state of a gaseous outflow needs a period of time to respond to changes in the ionizing continuum [the recombination timescale  $t^*$ , e.g. Krolik & Kriss (1995)]. Therefore, the gas ionization state is connected to the intensity of the ionizing continuum over  $t^*$ . It should be pointed out that the role of  $t^*$  is not a delay effect, but a smoothing effect. Absorption lines appear in the spectrum only when the ionized gas is situated along the line of sight. Consequently, there is no optical path difference between the absorption line and the intrinsic radiation, without any time delay. This characteristic makes it an ideal medium for studying the response of plasma to radiation sources. As illustrated in Fig. 1, the population density of a specific ion in the plasma initially increases to a peak and then decreases with the rise in ionization level. Hence, based on the peak

position, it can be classified into two stages: the low ionization state and the high ionization state. In the low ionization state, a positive correlation, termed a positive response, exists between the absorption line and the ionization source. Conversely, in the highly ionized state, the relationship is reversed.

Some studies (e.g., Wang et al. 2015; He et al. 2017) utilizing the large sample from Sloan Digital Sky Survey (SDSS) have revealed that over 70% of Si IV (ionization energy 45.1 eV), C IV (64.5 eV), N V (97.9 eV) broad absorption lines (BALs) exhibit a negative response. In other words, the majority of gases with variable BALs are in a highly ionized state. Naturally, there are some speculations regarding this. Does this negative response persist for ions with higher ionization energies, such as O VI (138.1 eV), or highly ionized iron (>1 keV)? Is it because most BAL gases are in a highly ionized state, or is there some physical asymmetry in the plasma that makes highly ionized ions more prone to responding to variations in the radiation source?

In this study, we explored the asymmetry of plasma response to radiation sources for low and high ionization states. Section 2 presents a comprehensive analysis of the asymmetry in plasma response time scales. In Section 3, we apply this asymmetry to C IV using photoionization simulation. The final section provides a summary.

## 2. THE ASYMMETRIC EFFECT OF RECOMBINATION-IONIZATION TIMESCALE

Here, we will provide an overview of the derivation process for the precise recombination timescale of the ionized gas in previous literature (e.g., Arav et al. 2012; Netzer 2013). The population density of a given element in ionization stage  $i$  is represented by

$$\frac{dn_i}{dt} = -n_i(I_i + R_{i-1}) + n_{i-1}I_{i-1} + n_{i+1}R_i, \quad (1)$$

where the ionization rate per particle is  $I_i$ , and the recombination rate per particle from ionization stage  $i+1$  to  $i$  is  $R_i$ . Here, we exclusively focused on the photoionization processes and omitted collisional ionization from our analysis. Equation 1 forms a set of  $n+1$  coupled differential equations for an element with  $n$  electrons and  $n+1$  ions. In the state of photoionization equilibrium, i.e., when  $dn_i/dt = 0$ , these reduce to  $n$  equations of the form

$$\frac{n_{i+1}}{n_i} = \frac{I_i}{R_i}. \quad (2)$$

This implies that the increase of stage  $i$  by recombination from stage  $i+1$  must be balanced by the decrease of stage  $i$  by ionization to stage  $i+1$ . For an optically thin gas at distance  $r$  from the radiation source with spectral luminosity  $L_\nu$  at frequency  $\nu$ , the ionization rate ( $s^{-1}$ ) per ion of stage  $i$  is given

by

$$I_i = \frac{\Gamma_i}{4\pi r^2}, \quad (3)$$

$\Gamma_i$  is the integral ionization cross-section rate ( $\text{cm}^2 \text{s}^{-1}$ ) over the photons with frequency  $\nu > \nu_i$ :

$$\Gamma_i = \int_{\nu_i}^{\infty} (L_\nu/h\nu)\sigma_\nu d\nu, \quad (4)$$

where  $h$  is Planck's constant and  $\sigma_\nu$  is the ionization cross-section for photons of energy  $h\nu$ . The  $\sigma_\nu$  for different atoms and ions can be obtained from the fitting formula in Equation 1 and Table 1 in (Verner et al. 1996). The recombination rate per particle is given by

$$R_i = \alpha_i(T)n_e, \quad (5)$$

where the recombination coefficient  $\alpha_i$  depends on the electron temperature  $T$  and scales roughly as  $T^{-1/2}$  (Osterbrock & Ferland 2006).

Suppose an absorber in photoionization equilibrium experiences a sudden change in the incident ionizing flux such that  $I_i(t > 0) = (1+f)I_i(t = 0)$ , where  $-1 \leq f \leq +\infty$ . Therefore, the change of ionization stage  $i$  can be written as:

$$\frac{dn_i}{dt} = -fn_iI_i + fn_{i-1}I_{i-1} = -fn_iI_i + fn_iR_{i-1}. \quad (6)$$

Then the characteristic timescale for change in the ionic fraction is:

$$t_i^* = \left[ -f\alpha_i n_e \left( \frac{n_{i+1}}{n_i} - \frac{\alpha_{i-1}}{\alpha_i} \right) \right]^{-1}, \text{ or} \quad (7)$$

$$= \left[ -f(I_i - n_e\alpha_{i-1}) \right]^{-1}. \quad (8)$$

As shown in Fig. 2, when the gas is in a sufficiently low ionization state, i.e.,  $n_{i+1}/n_i \ll \alpha_{i-1}/\alpha_i$  or  $I_i \ll n_e\alpha_{i-1}$ , the characteristic timescale is  $t_i^* = 1/(fn_e\alpha_{i-1})$ . On the contrary, when the gas is in a sufficiently high ionization state, i.e.,  $n_{i+1}/n_i \gg \alpha_{i-1}/\alpha_i$  or  $I_i \gg n_e\alpha_{i-1}$ , the characteristic timescale is  $t_i^* = -1/(f\alpha_i n_e \frac{n_{i+1}}{n_i}) = -1/(fI_i) = -r^2/(f\Gamma_i)$ . Note that a negative timescale indicates a decrease in  $n_i$  with time. Clearly, this timescale exhibits asymmetry for low ionization and high ionization states. In the low ionization state, the characteristic timescale is dominated by the recombination coefficient (i.e., the so-called recombination timescale), whereas in the high ionization state, it is dominated by the ionization rate. Hence, a more accurate term for the characteristic timescale in Equations 7, 8 should be the recombination-ionization timescale. In a highly ionized state, the  $t_i^*$  is shorter, that is, when the radiation source flux changes, the time required to return to gas ionization equilibrium is shorter.

In principle, an absorption line should vary from one observation to another only if both the time over which the ionizing continuum varies and the time interval  $\Delta T$  between the observations is longer than the  $t^*$ . This asymmetry suggests that in actual observations, the variations of absorption line in high ionization states (negative response) should be more easily detected than that in low ionization states (positive response). This happens to be consistent with actual observations, i.e., over 70% of BAL in quasar spectrum exhibit a negative response (Wang et al. 2015; He et al. 2017), based on large SDSS samples.

We have published a series of methods for measuring the  $t^*$  using the variation of absorption lines (e.g., He et al. 2019, 2022; Zhao et al. 2021). In the low ionization state, we can initially deduce the gas density  $n_e$  based on the measured  $t_i^* = 1/(fn_e\alpha_{i-1})$ . Subsequently, combined with the measured gas ionization parameters, we can determine the distance  $r$  from the gas to the central radiation source. Conversely, in the high ionization state, we can first deduce the distance  $r$  based on the measured  $t_i^* = -r^2/(f\Gamma_i)$ . Then, combined with the measured gas ionization parameters, we can obtain the gas density  $n_e$ . As an example, in the next section, we will specifically apply this asymmetry to the C IV BALs on the AGN spectrum.

### 3. THE RECOMBINATION-IONIZATION TIMESCALE OF C IV BAL ON THE AGN SPECTRUM.

#### 3.1. The recombination-ionization timescales of C IV BAL vary with gas ionization parameters.

According the Equation 7, the expression for the recombination-ionization timescale of C IV (i.e., C<sup>3+</sup>) is

$$t_{\text{CIV}}^* = \left[ -f\alpha_{\text{CIV}}n_e \left( \frac{n_{\text{CV}}}{n_{\text{CIV}}} - \frac{\alpha_{\text{CIII}}}{\alpha_{\text{CIV}}} \right) \right]^{-1}. \quad (9)$$

In our calculation, we assume a typical value of  $f = 0.1$  in the AGN light curve. Using the Chianti atomic database version 8.0 (Del Zanna et al. 2015), at a nominal temperature of  $2 \times 10^4$  K, the typical values of the recombination coefficients is  $\alpha_{\text{CIV}} = 5.3 \times 10^{-12} \text{cm}^{-3} \text{s}^{-1}$  (from C V to C IV) and  $\alpha_{\text{CIII}} = 2.1 \times 10^{-11} \text{cm}^{-3} \text{s}^{-1}$  (from C IV to C III).

The ionization parameter is defined as follows:

$$U = \frac{Q_{\text{H}}}{4\pi r^2 n_{\text{H}} c}, \quad (10)$$

where

$$Q_{\text{H}} = \int_{\nu_0}^{+\infty} \frac{L_{\nu}}{h\nu} d\nu \quad (11)$$

is the source emission rate of hydrogen-ionizing photons and  $h\nu_0 = 13.6$  eV is the ionization potential of  $H^0$  for ionization out of the 1-s ground state.  $c$  is the speed of light in

vacuum, and  $n_{\text{H}} \approx 0.83n_e$  is the hydrogen number density. In our simulation, We adopt the UV-soft SED (Dunn et al. 2010) typically used for high-luminosity radio-quiet quasars, as the SED of the radiation source. A standard solar metallicity was adopted for the gas. As shown in Fig. 3, the curves of recombination coefficients of C III and C IV and the ratio of population density  $n_{\text{CV}}/n_{\text{CIV}}$  as a function of ionization parameters  $U$  can be obtained from the photoionization simulations using Cloudy c17 (Ferland et al. 2017). As shown in Fig. 4, we calculate the value of the  $t^*(\text{CIV})$  at  $\log 10 U$  from -3 to 2 for  $n_{\text{H}} = 10^4 \text{cm}^{-3}$  and  $10^7 \text{cm}^{-3}$ , respectively, based on the curves of recombination coefficients of C III and C IV and the ratio of population density  $n_{\text{CV}}/n_{\text{CIV}}$ . In the low ionization state, the  $t^*(\text{CIV})$  is about 0.6 and 600 days for  $n_{\text{H}} = 10^4 \text{cm}^{-3}$  and  $10^7 \text{cm}^{-3}$ , respectively. In actual observations, the time interval  $\Delta T$  typically falls between 1 and 1000 days. For gas with density  $n_{\text{H}} = 10^4 \text{cm}^{-3}$ , only its highly ionized state response can be detected. Therefore, in this case, more negative responses are observed than positive responses, indicating detectable asymmetric effects. However, for gases with density  $n_{\text{H}} = 10^7 \text{cm}^{-3}$ , both low and high ionization responses can be detected, indicating that asymmetric effects cannot be detected or the detected asymmetric effects will be very weak. Based on the observed significant asymmetry of the C IV BAL response, we can infer that the density of a typical BAL outflow gas should not exceed  $10^7 \text{cm}^{-3}$ . Interestingly, so far, most measured gas densities of the BAL outflow are below  $10^7 \text{cm}^{-3}$  (Korista et al. 2008; Moe et al. 2009; Dunn et al. 2010; Borguet et al. 2013; Lucy et al. 2014; Chamberlain et al. 2015; Arav et al. 2018; Leighly et al. 2018; Hamann et al. 2019; Xu et al. 2019; Byun et al. 2022a,b, 2023).

For the sake of convenience in summarizing, we created a  $t^*(\text{CIV})$  map (Fig. 5) on the plane composed of  $\log 10 U$  (from -3 to 2) and  $\log 10 n_e$  (from 2 to 8). The four dashed lines in the figure represent contour lines for observation time intervals  $\Delta T = 1000, 100, 10,$  and  $1$  day, respectively. Below the respective dashed line, the observation time interval is smaller than the recombination-ionization timescale, i.e.,  $\Delta T < t_{\text{CIV}}^*$ , rendering it an unresponsive region. With observation time intervals of 1000, 100, 10, and 1 day, the lower density limits detectable for both low ionization and high ionization states are  $10^{3.8} \text{cm}^{-3}$ ,  $10^{4.8} \text{cm}^{-3}$ ,  $10^{5.8} \text{cm}^{-3}$ , and  $10^{6.8} \text{cm}^{-3}$ , respectively. On the one hand, given a fixed observational time intervals, the lower the density of the gas, the more challenging it is to detect the response of the low ionized state. In other words, it becomes easier to detect the asymmetry of the response. On the other hand, to detect the response asymmetry of higher density gases, a shorter observation time interval is required.

### 3.2. Derivation of density and distance of gas in low ionization and high ionization states

From Equations 7 and 8, it's evident that the approximation of recombination-ionization timescale  $t^*$  expressions differ significantly between low and high ionization state limits. Hence, employing the  $t^*$  for deriving the density and distance of gases may yield entirely different results. In the case of low ionization state, the density can be directly derived from the  $t^*$ :  $n_e = 1/(ft_{\text{CIV}}^* \alpha_{\text{CIII}})$ . Combining ionization parameters (Equations 10), the expression for distance is obtained as follows:  $r = (4\pi cU)^{-1/2} (1.2Q_{\text{H}} f t_{\text{CIV}}^* \alpha_{\text{CIII}})^{1/2}$ . In the case of high ionization state, the density cannot be derived separately from the  $t^*$ . According to Equation 10, the expression for electron density can be obtained as:  $n_e = \frac{1.2Q_{\text{H}}}{4\pi r^2 U c}$ . After incorporating it into the calculation formula of  $t^*$  in the high ionization state, we obtain  $t_{\text{CIV}}^* = 4\pi r^2 U c / (f \alpha_{\text{CIV}} \frac{n_{\text{CV}}}{n_{\text{CIV}}} 1.2Q_{\text{H}})$ . In the case of ionization equilibrium,  $\alpha_{\text{CIV}} \frac{n_{\text{CV}}}{n_{\text{CIV}}} = \frac{I_i}{n_e}$ . By examining Equations 5 and 10, it becomes apparent that  $I_i$  is proportional to  $U$ . Consequently,  $\alpha_{\text{CIV}} \frac{n_{\text{CV}}}{n_{\text{CIV}}}$  is also proportional to  $U$ . According to the Cloudy simulation, we find that  $\log_{10} [\alpha_{\text{CIV}} \frac{n_{\text{CV}}}{n_{\text{CIV}}}] = \log_{10} U - 9.5$ , where the unit of  $\alpha_{\text{CIV}}$  is  $\text{cm}^3 \text{s}^{-1}$ . Then, the expression for distance is as follows:

$$r = 9.5 \text{ pc} \left( \frac{Q_{\text{H}}}{10^{55} \text{ s}^{-1}} \right)^{0.5} \left( \frac{f}{0.1} \right)^{0.5} \left( \frac{t_{\text{CIV}}^*}{10 \text{ days}} \right)^{0.5} \quad (12)$$

From here, we can find that in highly ionized states, distance measurement becomes simpler and no longer depends on specific ionization parameter values.

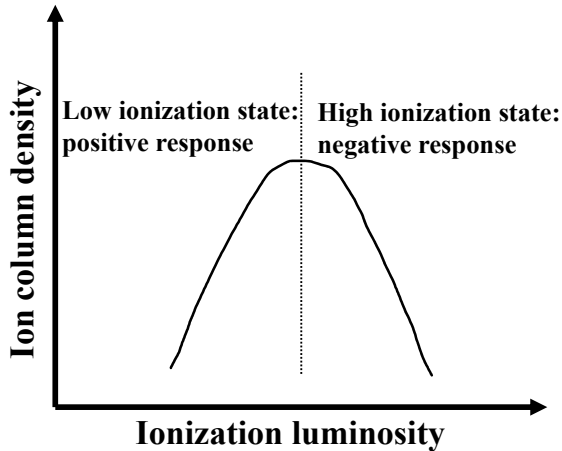


**Figure 1.** Schematic diagram of the variation of ion column density with ionization luminosity. The column density of a specific ion in the plasma initially increases to a peak and then decreases with the rise in ionization level. The vertical dashed line represents the peak position. Hence, based on the peak position, it can be classified into two stages: the low ionization state and the high ionization state.

### The asymmetric effect of response timescale

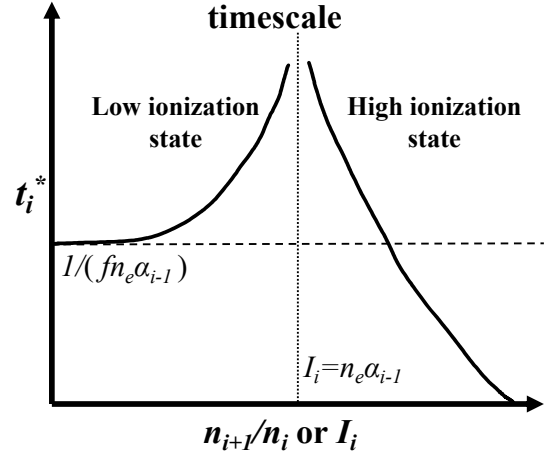


**Figure 2.** Schematic diagram of the asymmetric effect of ion response timescale. The vertical dashed line is the boundary between the low ionized state and the high ionized state. In a sufficiently low ionization state, i.e.,  $n_{i+1}/n_i \ll \alpha_{i-1}/\alpha_i$  or  $I_i \ll n_e \alpha_{i-1}$ , the characteristic timescale is  $t_i^* = 1/(fn_e \alpha_{i-1})$ . On the contrary, in a sufficiently high ionization state, i.e.,  $n_{i+1}/n_i \gg \alpha_{i-1}/\alpha_i$  or  $I_i \gg n_e \alpha_{i-1}$ , the characteristic timescale is  $t_i^* = -1/(f \alpha_i n_e \frac{n_{i+1}}{n_i}) = -1/(f I_i)$ . In highly ionized state, the response timescale is shorter than that of low ionized state, leading to the detection of more negative responses.

## 4. SUMMARY

Plasma stands out as one of the most prevalent forms of matter in the universe. It can serve as a valuable tool for scrutinizing the evolution of the cosmos. Simultaneously, plasma acts as an ideal laboratory for probing the properties of matter in extreme conditions, such as exceedingly high temperatures or low densities. As one of the significant contributors to the re-ionization of the universe, the variability in quasar radiation provides a convenient opportunity to study the response of ionized gases. Generally categorized into two stages—low ionization and high ionization—the response of plasma varies. In the low ionization state, a positive correlation, termed a positive response, exists between the absorption line and the ionization source. Conversely, in the highly ionized state, the relationship is reversed. Large-scale statistical analyses from the Sloan Digital Sky Survey (SDSS) have unveiled an intriguing asymmetry in the response of gases to quasar radiation—specifically, over 70% of BAL gases in quasar host galaxies exhibit a negative response.

In this work, we investigate whether there is a physical asymmetry effect in the plasma that makes highly ionized ions more responsive to changes in quasar radiation. Our results are as follows:

1, through analytical calculations and photoionization simulations of CIV, we have confirmed that the response of gases to radiation is asymmetric for low and high ionization states. In a sufficiently low ionization state, i.e.,  $n_{i+1}/n_i \ll$

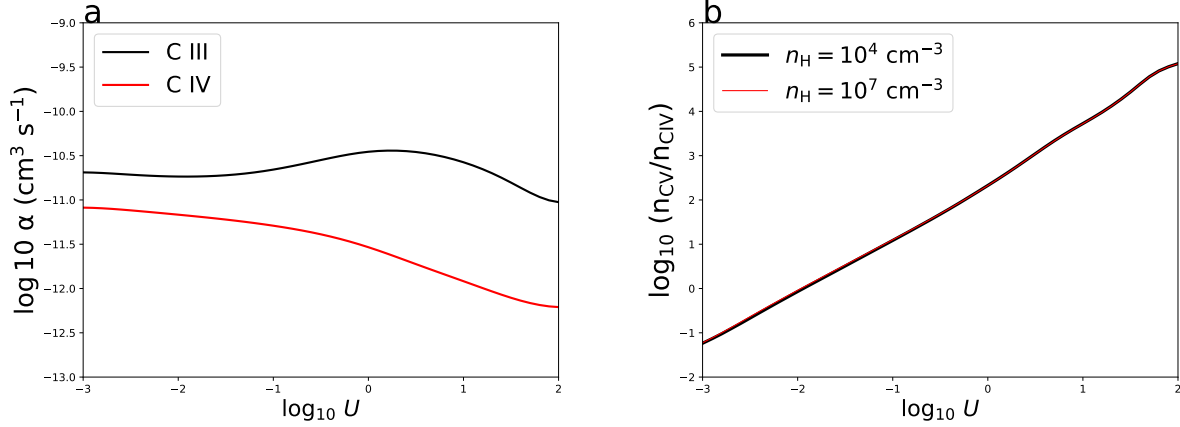


**Figure 3.** The recombination coefficients of C III and C IV, along with the ratio of population density  $n_{\text{CV}}/n_{\text{CIV}}$  under different ionization parameters, were obtained from photoionization simulations using Cloudy c17 (Ferland et al. 2017).

$\alpha_{i-1}/\alpha_i$  or  $I_i \ll n_e \alpha_{i-1}$ , the characteristic timescale is  $t_i^* = 1/(fn_e \alpha_{i-1})$ . On the contrary, in a sufficiently high ionization state, i.e.,  $n_{i+1}/n_i \gg \alpha_{i-1}/\alpha_i$  or  $I_i \gg n_e \alpha_{i-1}$ , the characteristic timescale is  $t_i^* = -1/(f\alpha_i n_e \frac{n_{i+1}}{n_i}) = -1/(fI_i) = -r^2/(fT_i)$ . In the low ionization state, the characteristic timescale is dominated by the recombination coefficient, whereas in the high ionization state, it is dominated by the ionization rate. In high ionization states, the response timescale is shorter, leading to the detection of more negative responses.

2, photoionization simulation shows that the recombination timescale range of C IV in low ionized states is 1-1000 days when the gas density ranges from  $10^7$  to  $10^4 \text{ cm}^{-3}$ . In actual observations, the time interval  $\Delta T$  typically falls between 1 and 1000 days. So, the asymmetry effect observed in C IV BALs during the observation time interval implies that the majority of BAL gas densities are below  $10^7 \text{ cm}^{-3}$ . Interestingly, this is consistent with the fact that most of the measured BAL gas densities are below  $10^7 \text{ cm}^{-3}$ . The lower

the plasma density or the shorter the observation time interval, the easier it is to detect this asymmetric effect.

3, we find that in highly ionized states, distance measurement becomes simpler and no longer depends on specific ionization parameter values.

The asymmetry of plasma response is only one possible explanation for the observed excessive negative response. To fully understand the the observed excessive negative response of absorption line gases to the variation radiation, it is essential to investigate whether this negative response can persist to ions with higher ionization energies, e.g., O VI (138.1 eV), or even highly ionized iron (>1 keV) in the future. Additionally, another important object for testing this asymmetric effect is the absorption lines generated by stellar winds (Lamers & Cassinelli 1999) in the stellar spectrum.

#### ACKNOWLEDGMENTS

Zhicheng He is supported by the National Natural Science Foundation of China (nos. 12222304, 12192220, and 12192221).

#### REFERENCES

- Arav, N., Liu, G., Xu, X., et al. 2018, *Astrophys. J.*, 857, 60
- Arav, N., Edmonds, D., Borguet, B., et al. 2012, *Astron. Astrophys.*, 544, A33
- Barkana, R., & Loeb, A. 2001, *Physics reports*, 349, 125
- Borguet, B. C., Arav, N., Edmonds, D., Chamberlain, C., & Benn, C. 2013, *Astrophys. J.*, 762, 49
- Byun, D., Arav, N., & Hall, P. B. 2022a, *Monthly Notices of the Royal Astronomical Society*, 517, 1048
- Byun, D., Arav, N., Sharma, M., Dehghanian, M., & Walker, G. 2023, arXiv preprint arXiv:2310.06216
- Byun, D., Arav, N., & Walker, A. 2022b, *Monthly Notices of the Royal Astronomical Society*, 516, 100
- Chamberlain, C., Arav, N., & Benn, C. 2015, *Mon. Not. R. Astron. Soc.*, 450, 1085
- Del Zanna, G., Dere, K., Young, P., Landi, E., & Mason, H. 2015, *Astron. Astrophys.*, 582, A56
- Dunn, J. P., Bautista, M., Arav, N., et al. 2010, *Astrophys. J.*, 709, 611
- Fabian, A. C. 2012, *Annual Review of Astronomy and Astrophysics*, 50, 455
- Fan, X., Bañados, E., & Simcoe, R. A. 2023, *Annual Review of Astronomy and Astrophysics*, 61, 373
- Fan, X., Carilli, C., & Keating, B. 2006, *Annu. Rev. Astron. Astrophys.*, 44, 415

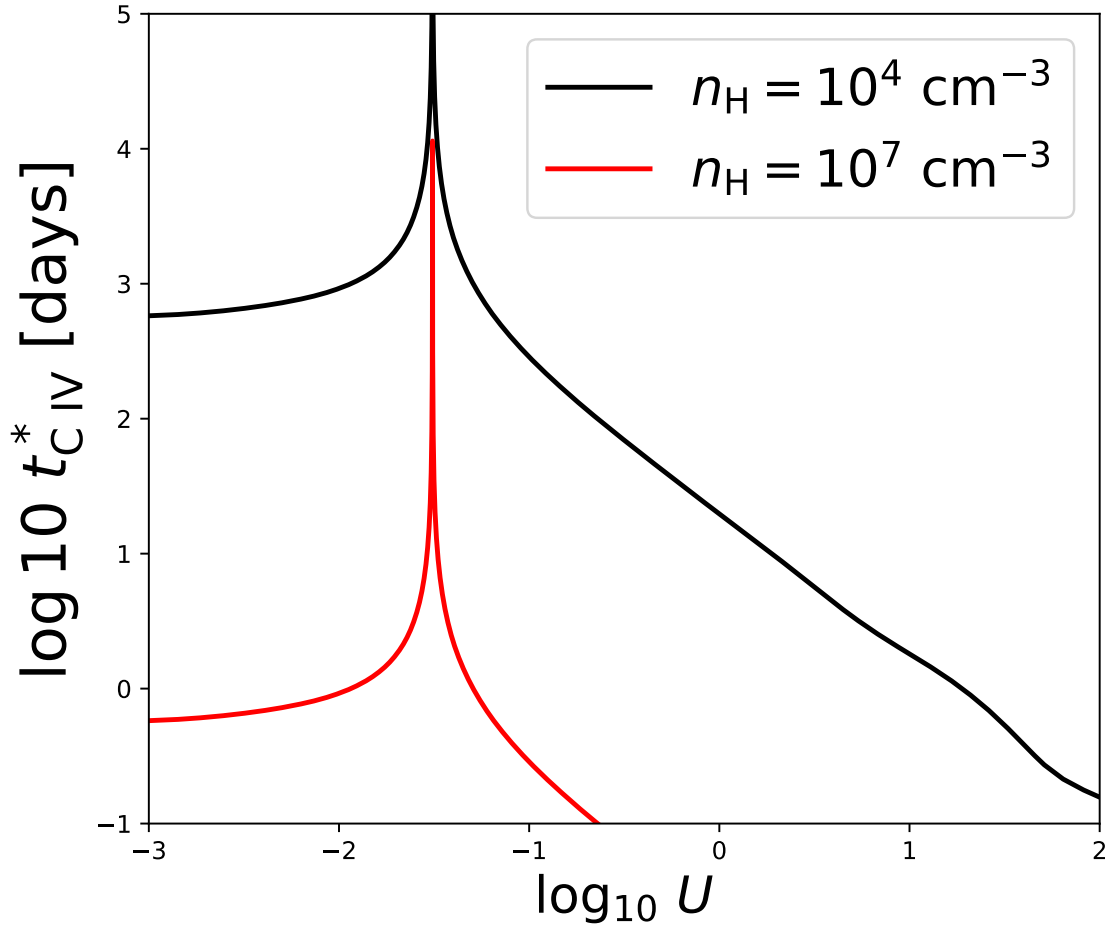


**Figure 4.** The recombination-ionization timescale curve of C IV under different ionization parameters. The black and red lines correspond to gas densities of  $10^4 \text{ cm}^{-3}$  and  $10^7 \text{ cm}^{-3}$ , respectively. The timescale is asymmetric, with the timescale of highly ionized states being much smaller than that of low ionized states. If the observation time interval is between 1-1000 days, we will not detect the response asymmetry of gas with a density of  $10^7 \text{ cm}^{-3}$ , but we can detect the response asymmetry of gas with a density of  $10^4 \text{ cm}^{-3}$ .

Ferland, G., Chatzikos, M., Guzmán, F., et al. 2017, *Revista mexicana de astronomía y astrofísica*, 53

Hamann, F., Herbst, H., Paris, I., & Capellupo, D. 2019, *Monthly Notices of the Royal Astronomical Society*, 483, 1808

He, Z., Wang, T., Zhou, H., et al. 2017, *Astrophys. J. Suppl. Ser.*, 229, 22

He, Z., Wang, T., Liu, G., et al. 2019, *Nature Astronomy*, 3, 265

He, Z., Liu, G., Wang, T., et al. 2022, *Science advances*, 8, eabk3291

Jakobsen, P., Boksenberg, A., Deharveng, J., et al. 1994, *Nature*, 370, 35

Kelly, B. C., Bechtold, J., & Siemiginowska, A. 2009, *The Astrophysical Journal*, 698, 895

Korista, K. T., Bautista, M. A., Arav, N., et al. 2008, *ApJ*, 688, 108

Kormendy, J., & Ho, L. C. 2013, *Annual Review of Astronomy and Astrophysics*, 51, 511

Kriss, G., Shull, J., Oegerle, W., et al. 2001, *Science*, 293, 1112

Krolik, J. H., & Kriss, G. A. 1995, arXiv preprint astro-ph/9501089

Lamers, H. J., & Cassinelli, J. P. 1999, *Introduction to stellar winds* (Cambridge university press)

Leighly, K. M., Terndrup, D. M., Gallagher, S. C., Richards, G. T., & Dietrich, M. 2018, arXiv:1808.02441

Loeb, A., & Barkana, R. 2001, *Annual review of astronomy and astrophysics*, 39, 19

Lucy, A. B., Leighly, K. M., Terndrup, D. M., Dietrich, M., & Gallagher, S. C. 2014, *The Astrophysical Journal*, 783, 58

Moe, M., Arav, N., Bautista, M. A., & Korista, K. T. 2009, *Astrophys. J.*, 706, 525

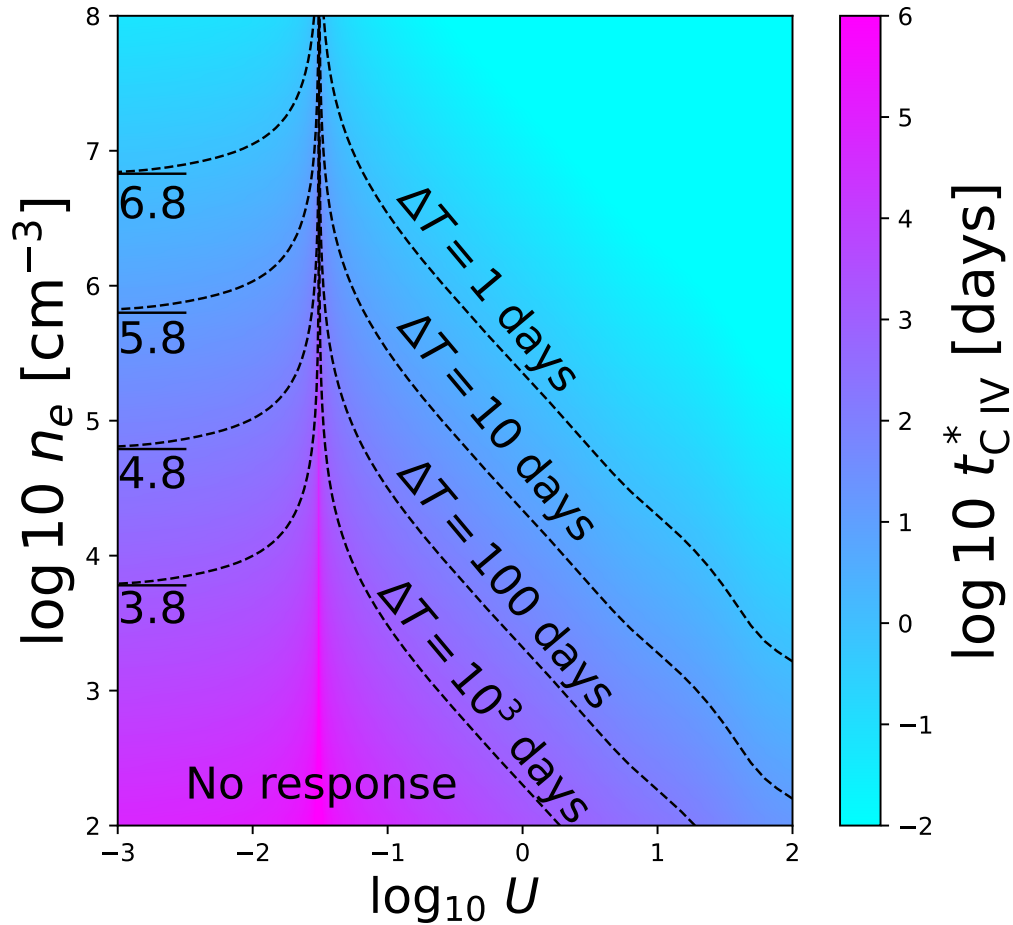


**Figure 5.** The map of C IV recombination-ionization timescales on the plane composed of ionization parameter and gas density. The dashed lines are the contours observed at intervals  $\Delta T$  of 1, 10, 100 and 1000 days. Below each contour line, the observation time interval is smaller than the recombination-ionization timescale, resulting in a non-responsive region.

Netzer, H. 2013, *The physics and evolution of active galactic nuclei* (Cambridge university press)

Osterbrock, D. E., & Ferland, G. J. 2006, *Astrophysics of gaseous nebulae and active galactic nuclei*, 2nd, University Science Books, Sausalito, CA

Tilvi, V., Malhotra, S., Rhoads, J., et al. 2020, *The Astrophysical Journal Letters*, 891, L10

Veilleux, S., Maiolino, R., Bolatto, A. D., & Aalto, S. 2020, *The Astronomy and Astrophysics Review*, 28, 1

Verner, D., Ferland, G., Korista, K., & Yakovlev, D. 1996, *Astrophysical Journal*, 465

Wang, F., Yang, J., Fan, X., et al. 2021, *The Astrophysical Journal Letters*, 907, L1

Wang, T., Yang, C., Wang, H., & Ferland, G. 2015, *Astrophys. J.*, 814, 150

Xu, X., Arav, N., Miller, T., & Benn, C. 2019, *The Astrophysical Journal*, 876, 105

Yung, L. A., Somerville, R. S., Finkelstein, S. L., et al. 2020, *Monthly Notices of the Royal Astronomical Society*, 496, 4574

Zhao, Q., He, Z., Liu, G., et al. 2021, *The Astrophysical Journal Letters*, 906, L8

Zheng, W., Kriss, G., Deharveng, J.-M., et al. 2004, *The Astrophysical Journal*, 605, 631